Cosmogenic ^{11}C production and sensitivity of organic scintillator detectors to *pep* and CNO neutrinos

Cristiano Galbiati* and Andrea Pocar†
Physics Department, Princeton University, Princeton, New Jersey 08544

Davide Franco‡
Dipartimento di Fisica, Università degli Studi di Milano, I-20133 Milano, Italy

Aldo Ianni
Laboratori Nazionali del Gran Sasso, I-67010 Assergi, Italy

Laura Cadonati
Physics Department, Massachusetts Institute of Technology, Cambridge, Massachusetts 02139

Stefan Schönert
Max-Planck-Institut für Kernphysik, D-69117 Heidelberg, Germany
(Received 8 November 2004; published 20 May 2005)

Several possible background sources determine the detectability of *pep* and CNO solar neutrinos in organic liquid scintillator detectors. Among such sources, the cosmogenic ^{11}C nuclide plays a central role. ^{11}C is produced underground in reactions induced by the residual cosmic muon flux. Experimental data available for the effective cross section for ^{11}C by muons indicate that ^{11}C will be the dominant source of background for the observation of *pep* and CNO neutrinos. ^{11}C decays are expected to total a rate 2.5 (20) times higher than the combined rate of *pep* and CNO neutrinos in Borexino (KamLAND) in the energy window preferred for the *pep* measurement between 0.8 and 1.3 MeV. This study examines the production mechanism of ^{11}C by muon-induced showers in organic liquid scintillators with a novel approach: for the first time, we perform a detailed *ab initio* calculation of the production of a cosmogenic nuclide, ^{11}C, taking into consideration all relevant production channels. Results of the calculation are compared with the effective cross sections measured by target experiments in muon beams. This article also discusses a technique for reduction of background from ^{11}C in organic liquid scintillator detectors, which allows to identify on a one-by-one basis and remove from the data set a large fraction of ^{11}C decays. The background reduction technique hinges on an idea proposed by Martin Deutsch, who suggested that a neutron must be ejected in every interaction producing a ^{11}C nuclide from ^{12}C. ^{11}C events are tagged by a threefold coincidence with the parent muon track and the subsequent neutron capture on protons.

DOI: 10.1103/PhysRevC.71.055805 PACS number(s): 25.30.Mr, 25.20.−x, 26.65.+t, 96.40.Tv

I. INTRODUCTION

Observation of solar neutrinos over the past 35 years via seven experiments has offered a unique opportunity to probe particle physics beyond the standard model of electroweak and strong interactions and physics of the stellar models. Radiochemical experiments have measured the combined flux of a number of different neutrino sources [1–4]. The only solar neutrinos targeted by a real-time measurement thus far have been the ^{8}B neutrinos above a detection threshold of about 5 MeV [5–7]. Plans are in place to measure the neutrino spectrum below 1 MeV with organic liquid scintillator-based detectors, focusing on the presumably abundant ^{7}Be neutrinos, with Borexino [8], KamLAND [9], and a possible detector at SNOLab [10]. Such detectors also have the potential to probe the intermediate energy region, searching for the less abundant *pep* and CNO neutrinos.

The possibility of detecting *pep* neutrinos in organic liquid scintillator based detectors is particularly intriguing. It was recently pointed out [11] that a measurement of the flux of *pep* solar neutrinos would yield essentially equivalent information about neutrino oscillation parameters and the other solar neutrino fluxes as a measurement of *pp* solar neutrinos at a comparable level of experimental uncertainty. Moreover, given the low theoretical uncertainty on the *pep* neutrinos flux, its measurement could allow investigating the matter-vacuum transition region for solar neutrino oscillations [11]. We recall that a transition from the matter-dominated to the vacuum-dominated region of solar neutrino oscillations is expected in the region between 2 and 3 MeV for the Mikheyev-Smirnov-Wolfenstein (MSW) matter enhanced oscillations Large Mixing Angle (LMA) solution [12] of the solar neutrino problem. Because of this transition, the survival probability (i.e., the probability that electron neutrinos emitted by the sun

*Corresponding author. E-mail address: galbiati@princeton.edu
†Now at Physics Department, Stanford University, Stanford, California 94305.
‡Also at Max-Planck-Institut für Kernphysik, Heidelberg D 69117, Germany.

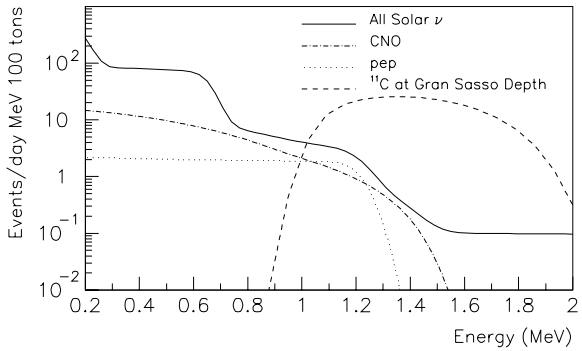

FIG. 1. Energy spectrum of electrons scattered by *pep* (dotted line) and CNO neutrinos (dash-dotted line), for the MSW-LMA solution of the solar neutrino problem. The total spectrum for all solar neutrinos (including *pp*, ^{7}Be, and ^{8}B neutrinos, not shown separately) is also shown (continuous line). Neutrino fluxes for the spectra shown are from the BP04 version of the standard solar model (see Ref. [11]). The background signal expected from cosmogenic ^{11}C at Gran Sasso depth is superimposed (dashed line). For all the neutrino and the ^{11}C spectra, we assume that the energy resolution of the detector is 5% at 1 MeV and varies with the energy E as $1/\sqrt{E}$.

have not oscillated into other neutrino species when they arrive on earth) for *pep* neutrinos is about a factor of two larger than the one measured at higher energy by the SNO experiment for ^{8}B neutrinos [5]. The measurement of the *pep* neutrinos flux would thus provide a further stringent test of the MSW-LMA solution.

The interaction rates for *pep* and CNO solar neutrinos in organic scintillator predicted by the BP04 version of the standard solar model by Bahcall and Pinsonneault [13], in the currently preferred MSW-LMA solution for the solar neutrino problem [11], are 2.1 and 6.6 events per day in 100 metric tons of liquid scintillator respectively. When data recently released by the LUNA collaboration for the ^{14}N+p fusion cross section [14] are taken into consideration, the signal rate from CNO neutrinos is significantly decreased to an expected 3.5 events per day in 100 tons.

The *pep* neutrino energy spectrum is distinctive, with a single 1.44-MeV monochromatic line. The energy spectrum for electrons scattered in ν-e interactions presents a characteristic Compton-like edge at 1.22 MeV. Figure 1 shows the expected (MSW-LMA) spectrum of scattered electrons from different neutrino sources in the energy range of interest for this study. We focus our attention on the detection and measurement of the *pep* neutrino line. For this purpose we set an observation window for the recoil electron between 0.8 and 1.3 MeV: for sake of simplicity, all event rates cited in the following will refer to this energy window, unless otherwise noted. The expected signal rate S in said window for *pep* and CNO neutrinos combined is 2.0 events per day in 100 tons (1.5 events per day per 100 tons when using the most recent results from LUNA). There are three fundamental prerequisites for a succesful measurement of the *pep* and CNO solar neutrinos in an organic liquid scintillator detector.

First, the internal background from long-lived radioactive sources must be carefully controlled. A ^{238}U and ^{232}Th contamination at the 10^{-17} g/g level, coupled with a $^{\text{nat}}$K contamination of 10^{-15} g/g, would produce 0.6 background events per day in 100 tons in the observation window [8,15]; this is below the event rate expected for *pep* neutrinos. Contamination from long-lived radon daughters out of secular equilibrium with ^{238}U (in particular from ^{210}Bi) must also be reduced below one count per day in the window of interest [8,9,16].

A second prerequisite is a low external γ-ray background from the construction materials of the detector and from the surrounding rocks. The general strategy to solve the problem is to use pure buffer materials to screen environmental radioactivity present in underground laboratories [8] and extremely low radioactivity construction materials [17]. The typical spherical geometry of liquid scintillator-based detectors has a peculiar effect on the spectrum of γ-induced events reconstructed within a given radius: the spectrum gets harder at smaller radii. Therefore, in the innermost part of the detector the γ-ray-induced background in the *pep* window (0.8–1.3 MeV) is larger than the corresponding background in the ^{7}Be window (0.25–0.8 MeV). This potential problem may be counterbalanced by redefining the fiducial mass for the observation of *pep* and CNO neutrinos. For reference, in the 100 tons fiducial mass of Borexino for ^{7}Be neutrinos detection the external background in the (0.8–1.3 MeV) window is expected at 1 event per day [8,15] compared with a neutrino signal of 2.0 events per day. Reducing the mass to 70 tons would lower the background by a factor 10 while losing only 30% of the signal [8,15].

The third fundamental condition for the observation of *pep* and CNO neutrinos is a low internal cosmogenic background production. This topic is the main subject of this article. Section II is an introduction to the problem of ^{11}C cosmogenic background in liquid scintillator detectors. Section III describes the production channels for cosmogenic ^{11}C and the results of our calculations for the expected production rate in a 100 tons liquid scintillator target. Section IV offers a comparison of our calculation with another estimate available in the literature for the production of ^{11}C by direct interaction of a muon with a ^{12}C nucleus through virtual photons. Finally, Sec. V proposes a reduction technique for ^{11}C production events, based on the double coincidence with the parent muon and a neutron produced in the reaction. We draw our conclusions in Sec. VI.

II. COSMOGENIC BACKGROUND IN DEEP UNDERGROUND DETECTORS

Cosmogenic radioactive nuclides are produced in deep underground detectors in reactions triggered by the residual muon flux. As originally pointed out in Ref. [18], the fundamental scale of the process is given by the neutron production rate: neutrons are an important and ubiquitous by-product of cosmic-ray-induced nuclear reactions.

A comprehensive review of the experimental results on neutron production in underground laboratories can be found in Ref. [19]. The first measurement at Gran Sasso (depth of 3800 m of water equivalent, muon flux of 1.2 m^{-2} hr^{-1}, average muon energy 320 GeV [20]) was performed with the

TABLE I. Depth (D), residual muon flux (Φ_μ), average muon energy ($\langle E_\mu \rangle$), neutron capture rate (N), and expected ^{11}C production rate (P) at KamLAND, Borexino, and SNOLab. Data on muons are from Refs. [9,20,24–28]. The neutron capture rate N for Borexino comes from the CTF experiment [8,21,22] and the one for KamLAND is the rate measured in the detector and reported in Ref. [9]. The neutron capture rate for SNO is obtained by extrapolating the CTF data with the scaling law ($N \propto \Phi_\mu \langle E_\mu \rangle^{0.7}$) first introduced in Ref. [18]; when the same procedure is applied to calculate the capture rate in KamLAND, the result of 294 cts/d 100 tons is fully consistent with the measured value. For the ^{11}C production rate P, data for Borexino and KamLAND are from Ref. [24], extrapolated from data of target experiment on muon beam at 100 and 190 GeV with the procedure also described in Sec. II. We calculated the value of P for SNOLab using the same extrapolation method of reference [24].

	Depth (m.w.e.)	Φ_μ (μ/m^2 h)	$\langle E_\mu \rangle$ (GeV)	N (cts/d 100 tons)	P (cts/d 100 tons)
KamLAND	2700	9.6	285	300	107
Borexino	3800	1.2	320	40	15
@ SNOLab	6000	0.012	350	0.43	0.15

Counting Test Facility (CTF) detector [16] in 1995 yielding $(1.5 \pm 0.1) \times 10^{-2}\, n/\mu$ m (neutrons per meter of muon track) in a trimethylbenzene- (C_9H_{12}) based scintillator with a density of 0.88 g/cm^3 [8,21,22]. A later measurement by the Large Volume Detector (LVD) experiment obtained $(1.4 \pm 0.4) \times 10^{-2}\, n/\mu$ m [23], always referred to the same density of 0.88 g/cm^3 that we will keep using as a reference throughout the article. The figure from the CTF experiment translates into a neutron capture rate of 40 events per day in 100 tons of scintillator.

Deutsch suggested [21] that the underground production rate for all of the most significant cosmogenic nuclides out of a target mass composed of ^{12}C and ^{1}H could be estimated from the neutron production rate alone. The list includes ^{8}Li, ^{9}Li, ^{11}Be, ^{8}B, ^{12}B, and ^{9}C, all with mean lives below 1 min and easily taggable with the parent muon. ^{7}Be is the cosmogenic radionuclide with the longest mean life, 77 days. ^{11}C also poses problems, given its 30-min mean life, which does not allow identification of its decays by tagging them with the parent muon alone. Deutsch hypothesized that ^{11}C would be one of the most likely cosmogenic nuclides by-products of muon-induced cascades and estimated that ^{11}C would account for 5% of the total neutron production rate. This would correspond to two events per day in the 100 fiducial tons of Borexino.

The inclusive cross sections for the production of several cosmogenic nuclides in muon-induced cascades were measured by a target experiment on a muon beam at CERN [24]. The experiment used a liquid scintillator target. The muon showers were built up in 240 cm of concrete and 200 cm of water used as absorbers and placed in front of the ^{12}C targets consisting in cells of a mineral-oil-based liquid scintillator very similar to those in use in Borexino and KamLAND. The results in Ref. [24] have shown that ^{7}Be is not among the most likely products of cosmic-ray-induced reactions: its production rate at Gran Sasso depth is expected to be less than 0.1 events per day in 100 tons. The authors of said experiment also reported the effective cross sections for inclusive ^{11}C production for muons: $\sigma = (576 \pm 45)\,\mu$b at 100 GeV and $\sigma = (905 \pm 58)\,\mu$b at 190 GeV. The use of two positively charged muon (μ^+) beams of 100 and 190 GeV allowed to extract information about the energy dependence of the inclusive cross sections: the authors reported that the effective cross section for ^{11}C production depends on the muon energy as in $\sigma \propto E_\mu^\alpha$, where $\alpha = 0.73 \pm 0.10$. This allows to extrapolate the effective cross section at higher energy, obtaining for muons of 320 GeV a value of 1320 μb or, equivalently, 52.6×10^{-4} nuclides/μ m in a trimethylbenzene-based scintillator with a density of 0.88 g/cm^3. The authors used the effective cross section to calculate the expected ^{11}C production rate P in Borexino and KamLAND as follows:

$$P = \Phi_\mu\, \rho\, \beta\, \sigma(\langle E_\mu \rangle), \tag{1}$$

where Φ_μ is the muon flux, ρ is the density of ^{12}C targets, and β is a correction factor that takes into account the effect of averaging over the muon energy spectrum, defined as follows:

$$\beta = \left\langle E_\mu^\alpha \right\rangle / \langle E_\mu \rangle^\alpha = 0.87. \tag{2}$$

The expected ^{11}C production rate in Borexino is 15 events per day in 100 tons. The rate is different for other locations because of the different muon fluxes and muon average energies. Muon fluxes and expected ^{11}C production rates in KamLAND, Borexino, and at SNOLab are summarized in Table I. From the value of signal rate and the values of the ^{11}C production rates one can quickly estimate that the background at SNOLab is sufficiently low to enable *pep* and CNO neutrinos observation without need of any cuts on ^{11}C.

^{11}C is a positron emitter with a 0.96 MeV end point. In a liquid scintillator detector the spectrum of ^{11}C falls in the spectral region between 1 and 2 MeV, because the γ rays from the positron annihilation are detected simultaneously with the energy deposited by the positron. Approximately 35% of its decays produce an event in the *pep* window (0.8–1.3 MeV). The raw background rate induced by ^{11}C decays in the *pep* window, B_0, is then defined as follows:

$$B_0 = 0.35\, P. \tag{3}$$

III. ^{11}C PRODUCTION IN MUON-INDUCED SHOWERS

Deutsch pointed out that the only way to create ^{11}C is to knock a neutron off the ^{12}C nucleus and suggested to look for

a neutron in the final state of the reaction; he emphasized the possibility of a threefold coincidence with the parent muon track and the neutron capture on protons in the scintillator to tag the ^{11}C events on a one-by-one basis [21]. Conversely, as suggested by Calaprice, there is also the possibility of creating a ^{11}C while ejecting a deuteron in a (p, d) exchange reaction. The (p, d) reaction would be an invisible channel for ^{11}C production because the nuclide produced through such process cannot be tagged with the threefold coincidence mentioned above. Similarly, reactions triggered by π mesons can also produce decays in invisible channels, as explained later.

Following is a list of the leading reactions that can produce ^{11}C, together with their cross section and references to specific studies. For all the reactions with a neutron in the final state, the energy threshold is ∼20 MeV (i.e., the neutron binding energy in ^{12}C).

^{12}C(γ, n)^{11}C [29]: The cross section for the γ-ray-induced process peaks at 7 mb around 23 MeV. The value of the cross section in the region of the peak is relatively large for an electromagnetic interaction because of the giant dipole resonance [30].

^{12}C(n, $2n$)^{11}C [31]: The cross section has a sharp peak (17 mb) around 33 MeV. At higher energies, we rely on the set of experimental data reported by Kim *et al*. [31] in the range 40–150 MeV, which is the only available for energies above 40 MeV. Those data are affected by a large experimental error, as high as 40%. As pointed out by the authors, their results disagree starkly with theoretical expectations which predict much lower values for the cross section in the same energy range [32]. Also, we assume that at energies higher than 150 MeV the cross section keeps the constant value attained in the range 70–150 MeV. Uncertainties in the knowledge of the cross section for this process represent the largest systematic error in our *ab initio* calculation of the rate of production of cosmogenic ^{11}C. We estimate that the systematic error attributable to this source could reach 50% of the production rate expected from the ^{12}C$(n, 2n)^{11}$C channel. All the other cross sections are known with a precision better than a few percent.

^{12}C(p, $p + n$)^{11}C [33]: The cross section reaches a peak value of 98 mb at 40 MeV and then it decreases to a plateau of 30 mb, constant up to 1 GeV.

^{12}C(p, d)^{11}C [34]: The cross section has a threshold of 16 MeV and has been measured at 52 and 65 MeV (15 and 10 mb, respectively). The only measurement available above 100 MeV tells us that the cross section is in the range of a few μb and therefore negligible.

^{12}C(π^-, $\pi^- + n$)^{11}C [35]: The cross section exhibits a broad peak centered around the (3,3) resonance for the pion-nucleon quasielastic interaction (see Dropesky *et al*. in Ref. [35]) with a value of 70 mb at 190 MeV. Data are available up to 550 MeV, and show that the cross section reaches a plateau above 400 MeV. We assume that the cross section keeps a constant value at higher energies.

^{12}C(π^+, $\pi + N$)^{11}C [35]: The cross section exhibits a broad resonance peak in the same region, reaching 45 mb around 160 MeV. Data are available up to 470 MeV and show that the cross section reaches a plateau above 350 MeV. We assume that the cross section keeps a constant value at higher energies. Contrarily to π^-, positive mesons do not necessarily produce a neutron in the final state: the N in the final case stands for nucleon and can be either a proton or a neutron. Because of the possibile charge exhcange occurring in the strong meson-nucleon interaction, the fragments in the final state can be either $(\pi^+ + n)$ or $(\pi^0 + p)$, the latter having a threshold of 13 MeV. No data are available on the relative composition of the final state, but it is expected from theoretical considerations (see Chivers *et al*. in Ref. [35]) that the frequency of the invisible channel, with a proton in the final state, should account for 2/3 of all the π^+-induced reactions. We rely on this assumption in our calculations.

^{12}C(e, $e + n$)^{11}C [36]: The direct interaction of electrons and positrons with a nucleus, through a virtual photon, is expected to have a small cross section, of the order of $\alpha\,(1/137)$ times the peak value of the cross section for real photons. The measured value of the cross section at 30 MeV is 15 μb. At higher energies, the cross section can be calculated using the von Weizsäcker approximation [37] as follows:

$$\sigma_e = \int M(\nu)\,\sigma_\gamma(\nu)\,d\nu \tag{4}$$

where σ_e is the cross section for the ^{11}C production induced by electrons, σ_γ is the cross section for ^{11}C production by real photons, ν is the energy of virtual photons, and M is the number of virtual photons. In case of high-energy, ultrarelativistic charged particles inducing nuclear reactions with low-momentum transfer, the number of virtual photons can be approximated by the following [38]:

$$M(\nu) = (\alpha/\pi\nu)\,[2\ln(E/m) - 1] \tag{5}$$

where E is the energy of the charged particle and m is its mass. The cross section for the production induced by electrons is then given by the following:

$$\sigma_e = (\alpha/\pi)\,[2\ln(E/m) - 1]\,\sigma_{-1} \tag{6}$$

where $\sigma_{-1} = \int d\nu\,\sigma_\gamma(\nu)/\nu$ is the inverse energy weighted moment of the photodisintegration cross section σ_γ. Using the photodisintegration cross sections from references [29], we calculated a value of 1.74 mb for σ_{-1}. With this value, the cross sections for the production of ^{11}C by electrons of 100 MeV, 1 GeV, and 10 GeV are 39 μb, 57 μb, and 76 μb respectively. The values of the cross sections at intermediate energies are interpolated from the above values.

^{12}C(μ, $\mu + n$)^{11}C: The direct interaction of muons with a nucleus, through a virtual photon, is usually referred to as "muon spallation." The cross section for the process can be calculated using the same procedure detailed above for electrons. The result is a cross section of 58 μb for muons at 320 GeV. In the range 100–350 GeV the cross sections have values very close to the one just quoted, given the

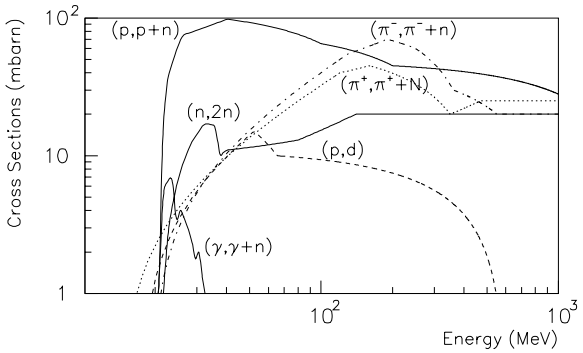

FIG. 2. Cross sections for ^{11}C production from ^{12}C as a function of energy.

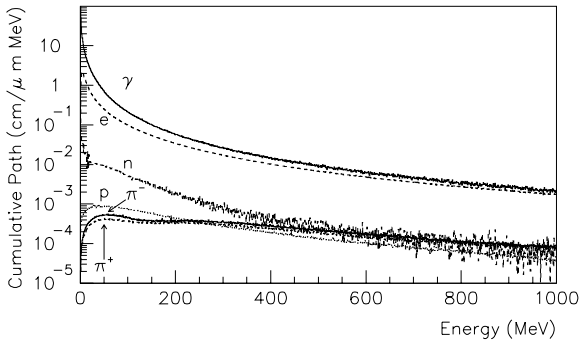

FIG. 3. Cumulative path of secondaries generated in showers induced by negatively charged muons at 320 GeV. Results are quoted in cm of range per meter of μ track per energy bins of 1 MeV.

logarithmic dependence of the number of virtual photons M upon the energy E, as shown in Eq. (5).

The cross sections for ^{11}C production by photons and hadrons, compiled using the procedure detailed above, are shown in Fig. 2.

We performed a full simulation of muon-induced showers with the particle transport code FLUKA [39]. The FLUKA code has been used by Wang *et al*. [19] to calculate the production rate of neutrons by muons in liquid scintillator at several depths and has been found to reproduce experimental results very well. Recently, FLUKA has been used by Kudryavtsev *et al*. [28] to calculate the distance between the parent muon track and the point of capture on protons of neutrons produced in scintillator by muon-induced cascades at Gran Sasso depth, and results were found to be in agreement with the experimental data from the LVD experiment [23].

We used FLUKA to calculate production rates, ranges, and paths of all the prominent secondaries (i.e., γ rays, electrons, neutrons, protons, and π mesons). We simulated showers originating from negatively charges muons (μ^-) at 100 and 190 GeV (the energies of the muon beams for the experiement described in Ref. [24]), at 285 GeV (average energy at Kamioka), at 320 GeV (average energy at Gran Sasso), and at 350 GeV (average energy at SNOLab). The target material in the simulation was the solvent of the liquid scintillator for Borexino, trimethylbenzene (C_9H_{12}), with density 0.88 g/cm^3 (incidentally, this makes up 20% of the solvent used in KamLAND [9]). Results should not vary greatly with other organic solvents, given that typical values of density and mass ratio between carbon and hydrogen are close to the values of trimethylbenzene. We tracked muons for 100 meters, and for each of the prominent secondaries we calculated the cumulative path of the particles as a function of the particle energy with a 10 GeV cutoff. The results for secondary particles with energy below 1 GeV in showers induced by negatively charged muons at 320 GeV are shown in Fig. 3.

We then turned to the computation of the ^{11}C production rate for each one of the interactions listed above, for each of the energies of the muons taken into consideration. The production rate has been calculated by taking the energy convolution, for each of the possible interactions, of the cross sections with the cumulative path of the secondary particles responsible for inducing that particular interaction. Results are summarized in Table II. The production rate in the invisible channels rate has been calculated by adding the rate from the ^{12}C$(p, d)^{11}$C reaction to 2/3 of the rate from the ^{12}C$(\pi^+, \pi + N)^{11}$C reaction.

The error quoted in Table II accounts for the systematic error, coming from two main sources. The most important source is the uncertainty in the knowledge of the cross section for the process ^{12}C$(n, 2n)^{11}$C. Our best estimate for the systematic error is 50% of the production rate in such channel, which is between 5 and 7% of the total production rate depending on the energy. We also make the conservative assumption that the systematic error associated with the cross sections used by FLUKA to calculate the range of the secondaries accounts for 5% of the total production rate. We combine the two as independent sources of error. The statistical error associated with our Monte Carlo calculation is 0.6% and is negligible with respect to the systematic error.

The total calculated rate is systematically 20% higher than the measured rates on a beam at 100 and 190 GeV, even though the values are still within twice the combined experimental and systematic uncertainties. A possible explanation for the systematic discrepancy is the difference in the geometry between the experiment and the simulation: in the beam experiment, the muon shower is built up in 240 cm of concrete and 200 cm of water placed in front of the scintillator target, whereas for our calculation we simulated the muon-induced interactions in a bulk scintillator volume. The calculated rates at 285, 320, and 350 GeV, although systematically higher than the extrapolated values, are still in good agreement with them when considering the systematic error.

We also calculated the production rates for positively charged muons (μ^+) at 320 GeV. The difference in the production of ^{11}C, for all of the channels considered, by μ^+ and μ^- at 320 GeV is within the statistical error of our Monte Carlo calculation. We conclude that the dependence of the inclusive cross section for ^{11}C production on the sign of the charge of the muons is negligible within the scope of the study presented in this article.

We took into account also the possibility of producing ^{11}C nuclides from the target nuclide ^{13}C, which has a natural isotopic abundance of 1.1% [40]. The contributions of channels such as ^{13}C$(\gamma, 2n)^{11}$C [41], ^{13}C$(\pi^+, d)^{11}$C [42], and ^{13}C$(p, t)^{11}$C [43] are negligible with respect to the

TABLE II. Production rates for ^{11}C in muon induced showers in trimethilbenzene (C_9H_{12}, 0.88 g/cm^3). The calculated total production rates are compared with the experimental values available at 100 and 190 GeV from Ref. [24], and with the extrapolated values at the mean muon energy for KamLAND and Borexino (also from Ref. [24]) and at SNOLab. The procedures used to determine the expected rate from the invisible channels and the systematic error affecting our calculation are outlined in the text.

E_μ (GeV)	100	190	285	320	350
Process			Rate ($10^{-4}/\mu$ m)		
^{12}C$(p, p+n)^{11}$C	1.8	3.2	4.9	5.5	5.6
^{12}C$(p, d)^{11}$C	0.2	0.4	0.5	0.6	0.6
^{12}C$(\gamma, n)^{11}$C	19.3	26.3	33.3	35.6	37.4
^{12}C$(n, 2n)^{11}$C	2.6	4.7	7.0	8.0	8.2
^{12}C$(\pi^+, \pi + N)^{11}$C	1.0	1.8	2.8	3.2	3.3
^{12}C$(\pi^-, \pi^- + n)^{11}$C	1.3	2.3	3.6	4.1	4.2
^{12}C$(e, e+n)^{11}$C	0.2	0.3	0.4	0.4	0.4
^{12}C$(\mu, \mu+n)^{11}$C	2.0	2.3	2.4	2.4	2.4
Invisible channels	0.9	1.6	2.4	2.7	2.8
Total	28.3	41.3	54.8	59.9	62.2
1σ systematic	1.9	3.1	4.4	5.0	5.2
Measured	22.9	36.0			
1σ experimental	1.8	2.3			
Extrapolated			48.4	52.6	56.2

corresponding rates for processes with the same incident particles on the target nuclide ^{12}C, owing to smaller cross sections and to the low natural isotopic abundance of ^{13}C.

As shown in Fig. 3, the particle content of muon-induced showers is, as expected [44], dominated by γ rays and electrons. Around 25 MeV, at the giant dipole resonance of ^{12}C where the cross section for γ rays is quite large, the cumulative range of γ rays is two to three orders of magnitude larger than the corresponding values for neutrons and four to five orders of magnitude larger than for other hadrons. As a consequence, the dominant process for the production of ^{11}C nuclides is the (γ, n) exchange reaction, accounting for $\sim$60% of the total production rate, even if the hadronic cross sections for the ^{11}C production are up to a factor 10 larger than the peak value for γ rays. Electrons are not as effective as γ rays because their cross section is lower by a factor α. Other hadronic channels with a neutron in the final state and the muon-induced photodisintegration, also carrying a neutron, account for an additional 35% of the total production rate. The rate of ^{11}C production in the two invisible channels, corresponding to the (p, d) and the $(\pi^+, \pi^0 + p)$ exhange reactions, accounts for only about 5% of the total production rate.

Deutsch's idea of eliminating the ^{11}C events by looking at the threefold coincidence turns out to be still valid even in presence of invisible channels: only one out of twenty ^{11}C nuclides is produced without a neutron in the final state. In Sec. V we will quantify the effectiveness of the ^{11}C background reduction technique based on the double muon+neutron tagging.

IV. COMPARISON WITH PREVIOUS ESTIMATES

O'Connell and Schima [45] calculated the production rate of several radioactive nuclides in carbon, oxygen, and argon targets, at sea level and at the depth of KamLAND, only for the photoproduction induced by the virtual photons associated with the muons. For the ^{11}C nuclide, they took into consideration only the channel ^{12}C$(\mu, \mu+n)^{11}$C, which results, in our estimate, in a 5% contribution to the total production rate. They estimated a production rate of ^{11}C of 15 events per day in 100 tons of carbon at the KamLAND depth or, scaling with the muon flux quoted in Table I, an equivalent cross section of 6.8×10^{-4} nuclides/μ m in trimethylbenzene based scintillators (0.88 g/cm^3) for muons at 285 GeV. Their result is to be compared with our estimate for the same channel reported in Table II, which amounts to 2.4×10^{-4} nuclides/μ m. The estimate of O'Connell and Schima is about 3 times higher than our estimate. The reason for the discrepancy lies in the value chosen for σ_{-1}, the inverse energy weighted moment of the photodisintegration cross section. The value of σ_{-1} quoted in Ref. [45] is 4.5 mb and is taken from a measurement of the inverse energy weighted moment of the photodisintegration cross section performed on a carbon target with a 1 GeV bremsstrahlung beam [46]. That value is not consistent with the main source for the photoneutron cross sections used elsewhere in the article of O'Connell and Schima, the *Atlas of photoneutron cross sections obtained with monoenergetic photons* [47]; this source offers two values for σ_{-1}, whose average is 1.65 mb, extrapolated from three different experiments which measured directly the (γ, n) cross section using monochromatic photons from $T(p, \gamma)$

reactions or from in-flight annihilation of positrons (see Ref. [47] and references cited therein). Direct measurements of photoneutron cross sections at the giant dipole resonance with monochromatic photons are intrinsically more precise than measurements of σ_{-1} using bremsstrahlung photons as the one reported in Ref. [46]. The value we calculated from the cross sections in use in this article is 1.74 mb, in excellent agreement with the best estimate from Ref. [47] and is about a factor 2.5 lower than the value reported in Ref. [46] and quoted in Ref. [45].

V. ^{11}C REDUCTION TECHNIQUES

As shown in the previous section, at least one neutron is produced in association with 95% of the ^{11}C nuclides. This fraction of the ^{11}C background can be lowered with the muon+neutron tagging. The remaining 5% cannot be reduced with this technique.

In order to suppress the ^{11}C background, one needs to identify the position and time of each neutron created by a muon-induced shower and then captured on protons in the scintillator. Neutron capture on protons results in the emission of a distinctive 2.2 MeV γ ray. In hydrocarbons, neutrons can also be captured on ^{12}C resulting in γ rays of combined energy 4.9 MeV [48]. The cross section for the capture on ^{12}C is $\sim$1% of the cross section for capture on protons [49]. Once the neutron capture time and position are known, one needs to apply a cut in space and time around every capture point. The events within a time t from the double muon+neutron coincidence and inside a sphere of radius r from the neutron capture point are rejected. This technique, originally suggested in Ref. [21], has recently been succesfully applied in the 4-ton prototype Counting Test Facility of Borexino [50].

The length of time t for which events are rejected should be set to a few times the mean life of ^{11}C. Note that the information carried by the neutron capture does not tell us about the position of the ^{11}C birthplace. Therefore, it is important to set the radius r of the spherical cut to a few times the average neutron range (note: the spatial resolution of multiton organic liquid scintillator detectors is typically 10 cm for the 2.2 MeV γ rays from neutron capture [8] and can be neglected with respect to the average neutron range). For this reason, we calculated with Monte Carlo methods the energy distribution of the neutrons produced in association with ^{11}C nuclides for Borexino, KamLAND, and at SNOLab. The calculation was performed using the relative weights for ^{11}C production in the different channels as determined for muons of 320 GeV. The procedure is correct for all the three locations because the relative weights for ^{11}C production in the different channels at 285 and 350 GeV are within 3% of the values at 320 GeV (see Table II). We used the resulting distribution, shown in Fig. 4, to source neutrons into FLUKA, calculating the distribution of the range of neutrons produced in association with ^{11}C, shown in Fig. 5.

The average energy of neutrons produced in association with ^{11}C is much lower than the average energy of all neutrons produced in muon-induced showers: this is because of the dominant production mechanism being the photoneutron

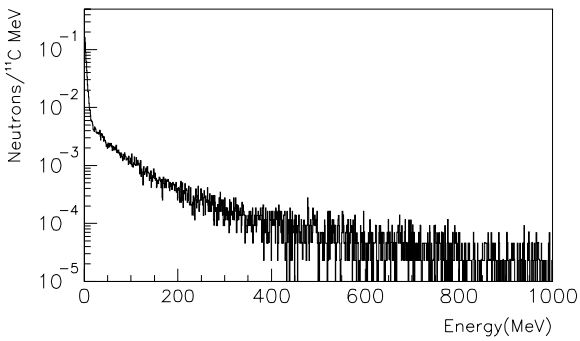

FIG. 4. Energy distribution for neutrons produced in association with ^{11}C nuclides.

reaction at the giant dipole resonance of ^{12}C at 23 MeV. Correspondingly, the average range of neutrons associated with ^{11}C production is also much lower than the average range of all the neutrons produced in the shower.

In our calculation we assumed that the ^{11}C nuclides displacement between the point where it is created and the point where it decays is negligible with respect to the range of neutrons created in association with the ^{11}C nuclides. For that to happen, the convective motion of the scintillator has to be sufficiently slow. This can be achieved, for example, by maintaining a small temperature gradient pointing upward everywhere in the detector. The average range of neutrons created in association with ^{11}C nuclides, whose distribution is shown in Fig. 5, is 44 cm. KamLAND data [51] show that the measured average displacement of the diffusive ^{222}Rn over its 5.5 days mean life is less than 1 m. Therefore the assumption that the ^{11}C nuclides displacement over their 30-min mean life can be kept small with respect to the neutrons range seems fully justified.

Because of the presence of the $(n, 2n)$ exchange reaction that yields two neutrons in the final state, an average of 1.14 neutrons are created in interactions producing ^{11}C nuclides. Those neutrons, if sufficiently energetic, can also trigger nuclear reactions knocking off other neutrons: our calculation indicates that an average number of about 1.2 neutrons are captured in the scintillator for each neutron produced in a ^{11}C-forming reaction.

The efficiency ϵ of rejecting ^{11}C events tagged with the muon+neutron coincidence is equal to the combined

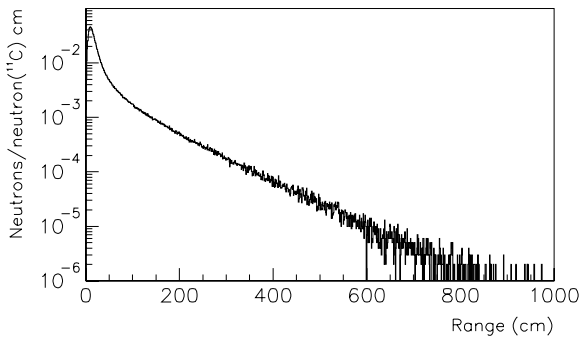

FIG. 5. Range of neutrons produced in association with ^{11}C nuclides.

efficiencies for the cut in space, $\zeta(r)$, and in time, $\eta(t)$, as follows:

$$\epsilon = \zeta(r)\,\eta(t), \tag{7}$$

where $\eta(t)$ is the efficiency for the rejection of ^{11}C events when a cut in time for a time span equal to t is applied around the neutron capture point. Given the expected decay distribution of ^{11}C, we obtain the following:

$$\eta(t) = 1 - e^{-t/\tau}, \tag{8}$$

where τ is the mean life of ^{11}C, 30 min.

In Eq. (7), $\zeta(r)$ is the rejection efficiency for ^{11}C when a cut in space is applied around the neutron capture point, corresponding to a sphere of radius r centered around the capture position. Given the distribution $n(s)$ for the range of neutrons shown in Fig. 5, the efficiency for the rejection is equal to the following:

$$\zeta(r) = \int_0^r n(s)\,ds \Big/ \int_0^\infty n(s)\,ds. \tag{9}$$

To quantify the effectiveness of the background reduction technique we introduce a figure of merit R, independent from the experiments and their locations. R is defined as the ratio of the *pep* + CNO neutrino signal rate (S) to the residual background rate (B) from ^{11}C after suppression of all ^{11}C events identified through the muon+neutron coincidence [both S and B are computed in the *pep* energy window (0.8–1.3 MeV)]. Note that the figure of merit R accounts only for the remaining background from ^{11}C, but other possible and independent sources of background are neglected in its definition. The general expression for R is as follows:

$$R = S/B = \frac{S/B_0}{F + (1-F)(1-\zeta\eta)}, \tag{10}$$

where $F \simeq 0.05$ is the fraction of ^{11}C production rate in invisible channels; S (signal rate) was discussed in Sec. I and B_0 (raw ^{11}C background rate, dependent on the location of the experiment) was discussed in Sec. II. Equations (7) and (10) show that there is a one-to-one correspondance between the figure of merit R and the combined rejection efficiency ϵ.

Using Eq. (10), we estimate that the optimal signal to background ratio achievable in Borexino (KamLAND) is 8:1 in case all of the ^{11}C associated with a neutron are successfully tagged. The optimal limit cannot, however, be reached because of dead mass-time limitations, as shown below.

We define the dead mass-time fraction D as the fraction of (mass × time) data taking lost to the space and time cuts around a neutron capture event. Treating η and ζ as independent variables, t and r can be derived by inverting Eqs. (8) and (9) and become functions of η and ζ respectively. We can then compute the dead mass-time fraction D corresponding to the chosen values of the cuts ζ and η as follows:

$$D = 1 - e^{-\frac{4}{3}\pi\rho r^3 t N}, \tag{11}$$

where ρ is the scintillator density and N is the neutron capture rate per unit mass in the detector. The expected neutron capture rates for the experiments taken into consideration are summarized in Table I.

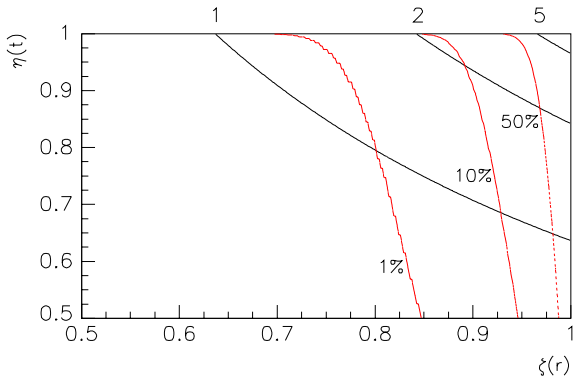

FIG. 6. (Color online) Correlation between the signal to reduced background ratio (R) and the dead mass-time fraction for Borexino, as a function of spatial (ζ) and time (η) efficiencies of ^{11}C events rejection. The only background considered in the *pep* energy window (0.8–1.3 MeV) is the ^{11}C background surviving the cuts described in the text. Isocontours for the ratio R (for values $R = 1, 2, 5$) and for the dead mass-time fraction D (for values $D = 1\%, 10\%, 50\%$) are shown in the graph.

Figure 6 shows the correlation between the signal to reduced background ratio R and the dead mass-time fraction D for Borexino, as a function of spatial (ζ) and time (η) efficiencies for ^{11}C events rejection. In Table III we show the optimal values of the dead mass-time fraction D for the three experiments for fixed and given values of the ratio R between signal and reduced ^{11}C background. The values are calculated by minimizing the dead mass-time fraction D while keeping the

TABLE III. Optimal values of the dead mass-time fraction (D) for KamLAND, Borexino, and at SNOLab as a function of the figure of merit R defined as the ratio between the signal rate (S) of *pep* and CNO neutrinos (BP04 model for MSW-LMA scenario [13]) and background rate (B) from ^{11}C after the reduction with the technique outlined in the text. In Borexino the ratio between signal rate and raw background before any ^{11}C rejection (B_0) is 0.4; in KamLAND, S/B_0 is 0.05; for a detector at SNOLab, S/B_0 would be 36.

S/B_0	0.05	0.4	36
$R = S/B$	KamLAND D [%]	Borexino D [%]	@ SNOLab D [%]
0.1	0.4		
0.2	11.6		
0.3	50.6		
0.4	87.4	<0.1	
0.5	98.8	<0.1	
0.8	>99.9	0.1	
1		0.3	
2		6.7	
3		27.8	
4		58.3	
5		85.3	
8		>99.9	
100			<0.1
500			2.6

product of the two efficiencies ζ, η constrained to the value of ϵ corresponding to the chosen value of R.

Further improvements of these figures might be achieved by the experiments by optimizing the set of cuts used to tag ^{11}C events with the double muon and neutron coincidence according to each detector's capabilities and performance. For example, the accurate reconstruction of the track of the through-going muons might help reducing the dead mass-time by modifying the topology of the spatial cut proposed in this study, such as limiting the volume of the region excluded by the cuts to an intersection of a cylinder around the muon track and of a sphere centered around the neutron capture point, as proposed in Ref. [50].

The technique offers as a by-product the possibility of determining the total number of ^{11}C decays in the detector. The residual background B can then be statistically subtracted from the spectrum of the reduced data set. Let T be the total rate in the *pep* window after applying the muon+neutron tagging technique. Under the assumption that the internal and the external background rates are negligible with respect to the residual background from ^{11}C and to the signal rates, $S = T - B$. A lower bound on the statistical error associated with the signal rate S extrapolated with the statistical subtraction of the energy spectra is obtained by propagating the errors in the formula just introduced:

$$\frac{\delta S}{S} = \frac{\sqrt{N_T + N_B}}{N_S} = \frac{\sqrt{N_S + 2N_B}}{N_S} = \sqrt{\frac{1 + 2/R}{SM(1 - D)t_0}}, \tag{12}$$

where N_T, N_S, and N_B are, respectively, the total number of events recorded, the total number of signal events and the total number of background events (all after application of the cuts to reduce the background from ^{11}C), t_0 is the data taking time and M is the fiducial mass for *pep* and CNO neutrinos observation. The formula above can be used to obtain information concerning the statistical accuracy of the measurement of the signal rate. Borexino (KamLAND) with a 70-ton (300-ton) fiducial mass would achieve a statistical accuracy of 2.9% (3.4%) in 5 years.

VI. CONCLUDING REMARKS

In this article we presented a study of the production mechanism of ^{11}C nuclides in muon-induced showers. We identified the nuclear reactions relevant for the production of the nuclide in muon-induced showers in organic liquid scintillators. We performed an *ab initio* calculation of the production rates for each channel and then compared the calculated total production rate with available experimental data, obtaining a good agreement. We estimated that for 95% of the ^{11}C nuclides produced at least one neutron is emitted.

A possible experiment located at SNOLab has a very low muon flux and hence a ^{11}C production rate that is negligible when compared with the expected rate from *pep* and CNO neutrinos. Conversely, for both Borexino and KamLAND, cosmogenic ^{11}C is a significant background for the detection of *pep* and CNO solar neutrinos.

We discussed a reduction technique for the ^{11}C events, based on one-by-one identification through the coincidence between a parent muon and the resulting neutron capture. We estimated that both Borexino and KamLAND could use the technique to increase the original signal (pep + CNO neutrinos) to background (^{11}C) ratio by a significant factor. Borexino can improve from a signal/background ratio of 0.4 to one of 2 (4) while losing 7% (58%) of the data to dead mass-time. KamLAND can improve its signal/background ratio from 0.05 to 0.2 (0.3) while losing 12% (51%) of data to dead mass-time.

The residual ^{11}C background can be statistically subtracted to determine the signal rate from neutrinos. We presented a formula providing a crude estimate of the statistical error associated with the signal rate determined with this procedure. We estimated that both Borexino and KamLAND could measure the combined rate from *pep* and CNO neutrinos in the (0.8–1.3 MeV) window down to a 3% statistical accuracy in 5 years, provided that internal and external background rates are kept within figures negligible with respect to the signal rate.

ACKNOWLEDGMENTS

We thank the late M. Deutsch, for inspiring discussions on the subject of cosmic-ray-induced interactions and for providing the founding idea behind this study. We thank F. Calaprice for useful discussions, for the suggestion to investigate all production channels, and for drawing our attention to the (p, d) exchange reaction. We thank C. Pe na-Garay and F. Vissani for reading the manuscript and for useful comments. We thank G. Battistoni for help in getting started with FLUKA simulations. The work of C.G. and A.P. was supported in part by the U.S. National Science Foundation under Grant PHY-0201141. L.C. acknowledges the support of the U.S. National Science Foundation under Grant PHY-0107417. C.G. acknowledges hospitality from the Dipartimento di Fisica of the Università degli Studi di Milano during part of this work.

[1] B. T. Cleveland *et al.*, Astrophys. J. **496**, 505 (1998).
[2] W. Hampel *et al.* (Gallex Collaboration), Phys. Lett. **B447**, 127 (1999).
[3] J. N. Abdurashitov *et al.* (Sage Collaboration), J. Exp. Theor. Phys. **95**, 181 (2002).
[4] M. Altmann *et al.* (GNO Collaboration), Phys. Lett. **B490**, 16 (2000).
[5] Q. R. Ahmad *et al.* (SNO Collaboration), Phys. Rev. Lett. **89**, 011301 (2002).
[6] K. S. Hirata *et al.* (Kamiokande-II Collaboration), Phys. Rev. D **44**, 2241 (1991).

[7] S. Fukuda *et al*. (Super-Kamiokande Collaboration), Phys. Rev. Lett. **86**, 5651 (2001).

[8] G. Alimonti *et al*. (Borexino Collaboration), Astropart. Phys. **16**, 205 (2002).

[9] K. Eguchi *et al*. (KamLAND Collaboration), Phys. Rev. Lett. **90**, 021802 (2003).

[10] M. Chen, in Proceedings of the NOW 2004 Conference, October 11–17 2004, Conca Specchiulla, Bari to be published in Nucl. Phys. B (Proc. Suppl.) See also slides of the talk at the NOW 2004 conference, available at http://www.ba.infn.it/∼now2004/.

[11] J. N. Bahcall and C. Peña-Garay, J. High Energy Phys. **11**, 004 (2003).

[12] L. Wolfenstein, Phys. Rev. D **17**, 2369 (1978); S. P. Mikheyev and A. Yu. Smirnov, Sov. J. Nucl. Phys. **42**, 913 1985.

[13] J. N. Bahcall and M. H Pinsonneault, Phys. Rev. Lett. **92**, 121301 (2004).

[14] A. Formicola *et al*., Phys. Lett. **B591**, 61 (2004).

[15] L. Cadonati, *The Borexino Solar Neutrino Experiment and Its Scintillator Containment Vessel*, Ph.D. thesis, Princeton University (2000).

[16] G. Alimonti *et al*. (Borexino Collaboration), Astropart. Phys. **8**, 141 (1998).

[17] C. Arpesella *et al*. (Borexino Collaboration), Astropart. Phys. **18**, 1 (2002).

[18] O. G. Ryazhskaya and G. T. Zatsepin, Izv. Akad. Nauk USSR, Ser. Fiz. **29**, 1946 (1965).

[19] Y-F. Wang *et al*., Phys. Rev. D **64**, 013012 (2001).

[20] M. Ambrosio *et al*. (MACRO Collaboration), Astropart. Phys. **10**, 11 (1999).

[21] M. Deutsch, *Proposal to NSF for a Borexino Muon Veto* (Massachusetts Institute of Technology, Cambridge, 1996).

[22] C. Galbiati, *Data Taking and Analysis of the Counting Test Facility of Borexino*, Tesi di Dottorato, Università degli Studi di Milano (1999).

[23] LVD Collaboration, M. Aglietta *et al*., *Measurement of the Neutron Flux Produced by Cosmic-Ray Muons with LVD at Gran Sasso*, Proceedings of the 26th International Cosmic Ray Conference, 1999, Salt Lake City, USA, Vol. 2, p. 44, preprint arXiv:hep-ex/9905047.

[24] T. Hagner *et al*., Astropart. Phys. **14**, 33 (2000).

[25] M. Cribier *et al*., Astropart. Phys. **6**, 129 (1997).

[26] C. Waltham *et al*., *Through-Going Muons in the Sudbury Neutrino Observatory*, Proceedings of the International Cosmic Ray Conference, Hamburg, 2001, edited by Copernicus Gesellschaft.

[27] N. Tagg, *The ^{8}Li Calibration Source and Through-Going Muon Analysis in the Sudbury Neutrino Observatory*, Ph.D thesis, University of Guelph (2001).

[28] V. A. Kudryavtsev, N. J. C. Spooner, and J. E. McMillan, Nucl. Inst. Methods A **505**, 688 (2003).

[29] L. Katz *et al*., Can. J. Phys. **29**, 518 (1951); L. D. Cohen and W. E. Stephens, Phys. Rev. **2**, 263 (1959); V. Emma, C. Milone, and A. Rubbino, *ibid*. **118**, 1297 (1960); J. P. Roalsvig *et al*., Can. J. Phys. **39**, 643 (1961); H. Fuchs *et al*., Zeit. Nat. A **17**, 439 (1962); W. E. Del Bianco *et al*., Phys. Rev. **126**, 709 (1962); V. V. Verbinski *et al*., Nucl. Phys. **73**, 398 (1965); W. A. Lochstet and W. E. Stephens, Phys. Rev. **141**, 1002 (1966); E. B. Bazhanov *et al*., Yad. Fiz. **3**, 711 (1966); H. Schier *et al*., Nucl. Phys. **A229**, 93 (1974); J. R. M. Annand *et al*., Phys. Rev. Lett. **71**, 2703 (1993).

[30] M. Goldhaber and E. Teller, Phys. Rev. **74**, 1046 (1948).

[31] J. E. Brolley Jr. *et al*., Phys. Rev. **88**, 618 (1952); O. D. Brill *et al*., Dok. Akad. Nauk SSR **136**, 55 (1961); F. Nasyrov *et al*., At. Energ. **25**, 437 (1968); P. J. Dimbylow, Phys. Med. Biol. **25**, 637 (1980); P. Welch *et al*., Bull. Am. Phys. Soc. **26**, 708 (1981); B. Anders *et al*., Zeit. Phys. A **301**, 353 (1981); T. S. Soewarsono *et al*., JAERI Tokai Rep. **27**, 354 (1992); Y. Uno *et al*., Nucl. Sci. Eng. **122**, 247 (1996); E. Kim *et al*., Nucl. Sci. Eng. **129**, 209 (1998).

[32] ENDF/B-VI, *Evaluated Nuclear Data File*, National Nuclear Data Center, Brookhaven National Laboratory (1990).

[33] J. B. Cumming, Phys. Rev. **111**, 1386 (1958); V. Parikh, Nucl. Phys. **18**, 628 (1960); P. A. Berioff, Phys. Rev. **119**, 316 (1960); N. Horwitz *et al*., Phys. Rev. **117**, 1361 (1960); K. Goebel *et al*., Nucl. Phys. **24**, 28 (1961); J. B. Cumming *et al*., Phys. Rev. **125**, 2078 (1962); H. Gauvin *et al*., Nucl. Phys. **39**, 447 (1962); G. W. Butler *et al*., Phys. Rev. C **6**, 1153 (1972); M. L. Barlett *et al*., Phys. Lett. **B264**, 21 (1991); D. S. Carman *et al*., Phys. Lett. **B452**, 8 (1999).

[34] P. G. Roos *et al*., Nucl. Phys. **A255**, 187 (1975); K. Hosono *et al*., Nucl. Phys. **A343**, 234 (1980); H. Ohnuma *et al*., J. Phys. Soc. Jpn. **48**, 1812 (1980); G. R. Smith *et al*., Phys. Rev. C **30**, 593 (1984).

[35] D. T. Chivers *et al*., Nucl. Phys **A126**, 129 (1969); K. R. Hogstrom *et al*., *ibid*. **A215**, 598 (1973); B. J. Dropesky *et al*., Phys. Rev. Lett. **34**, 821 (1975); M. M. Sternheim and R. R. Silbar, Phys. Rev. Lett. **34**, 824 (1975); B. J. Lieb, H. S. Plendl, C. E. Stronach, H. O. Funsten, and V. G. Lind, Phys. Rev. C **19**, 2405 (1979); J. F. Amann *et al*., Phys. Rev. Lett. **40**, 758 (1978).

[36] W. C. Barber, Phys. Rev. **111**, 1642 (1958); G. Kuhl and U. Kneissl, Nucl. Phys. **A195**, 559 (1972); E. Wolynec *et al*., Phys. Rev. C **11**, 1083 (1975); U. Kneissl, G. Kuhl, and K. H. Leister, Z. Phys. A **281**, 35 (1977); N. G. Shevchenko *et al*., Sov. J. Nucl. Phys. **28**, 5 (1978).

[37] C. F. von Weizsäcker, Z. Phys. **88**, 612 (1934); W. C. Barber and T. Wiedling, Nucl. Phys. **18**, 575 (1960); D. F. Herring *et al*., Phys. Rev. **139**, B562 (1965); W. W. Gargaro and D. S. Onley, *ibid*. **C4**, 1032 (1971); E. Wolynec *et al*., Nucl. Phys. **A244**, 205 (1975); I. C. Nascimento and E. Wolynec, *ibid*. **A246**, 210 (1975).

[38] R. H. Dalitz and D. R. Yennie, Phys. Rev. **105**, 1598 (1957); J. Delorme, M. Ericson, T. Ericson, and P. Vogel, Phys. Rev. C **52**, 2222 (1995).

[39] A. Fassò *et al*., *Electron-Photon Transport in FLUKA: Status*, Proceedings of the MonteCarlo 2000 Conference, Lisbon, October 23–26, 2000, edited by A. Kling, F. Barao, M. Nakagawa, L. Tavora, and P. Vaz (Springer-Verlag Berlin, 2001), p. 159; A. Fassò *et al*., *FLUKA: Status and Prospective for Hadronic Applications*, Proceedings of the MonteCarlo 2000 Conference, Lisbon, October 23–26, 2000, edited by A. Kling, F. Barao, M. Nakagawa, L. Tavora, and P. Vaz (Springer-Verlag Berlin, 2001) p. 955.

[40] *Table of Isotopes*, 7th edition, edited by C. M. Lederer and V. S. Shirley (Wiley-Interscience Publisher, New York, 1978).

[41] J. W. Jury *et al*., Phys. Rev. C **19**, 1684 (1979).

[42] K. G. R. Doss *et al*., Phys. Rev. C **25**, 962 (1982).

[43] S. W. Cosper *et al*., Phys. Rev. **176**, 1113 (1968); D. G. Fleming, J. Cerny, and N. K. Glendenning, *ibid*. **165**, 1153 (1968).

[44] D. E. Groom, N. V. Mokhov, and S. I. Striganov, At. Data Nucl. Data Tables **78**, 183 (2001).

[45] J. S. O'Connell and F. J. Schima, Phys. Rev. D **38**, 2277 (1988).
[46] V. di Napoli *et al*., Phys. Rev. C **8**, 206 (1973).
[47] B. L. Berman, At. Data Nucl. Data Tables **15**, 319 (1975); S. S. Dietrich and B. L. Berman, *ibid*. **38**, 199 (1988).
[48] R. C. Reedy and S. C. Frankle, At. Data Nucl. Data Tables **80**, 1 (2002).
[49] S. F. Mughabghab, M. Divadeenam, and N. E. Holden, *Neutron Cross Sections, Part A*, $Z = 1-60$, Academic Press (1981).
[50] D. Franco ford the Borexino Collaboration, *^{11}C Measurement and CNO Flux at Borexino*, Proceedings of the NOW 2004 Conference, October 11–17, 2004, Conca Specchiulla, Bari, to be published in Nucl. Phys. B (Proc. Suppl.). See also slides of the talk at the NOW 2004 conference, available at http://www.ba.infn.it/∼now2004/.
[51] J. Shirai for the KamLAND Collaboration, Nucl. Phys. (Proc. Suppl.) **B118**, 15 (2003); see also copies of slides of the talk at the Neutrino 2002 conference, available at http://neutrino2002.ph.tum.de/.